Three-dimensional visualization and a deep-learning model reveal complex fungal parasite networks in behaviorally manipulated ants

Maridel A. Fredericksen[a], Yizhe Zhang[b], Missy L. Hazen[c], Raquel G. Loreto[a,d], Colleen A. Mangold[d,e], Danny Z. Chen[b], and David P. Hughes[a,d,f,1]

[a]Department of Entomology, Pennsylvania State University, University Park, PA 16802; [b]Department of Computer Science and Engineering, University of Notre Dame, Notre Dame, IN 46556; [c]Huck Institutes of the Life Sciences Microscopy and Cytometry Facility, Pennsylvania State University, University Park, PA 16802; [d]Center for Infectious Disease Dynamics, Pennsylvania State University, University Park, PA 16802; [e]Department of Biochemistry and Molecular Biology, Pennsylvania State University, University Park, PA 16802; and [f]Department of Biology, Pennsylvania State University, University Park, PA 16802

Edited by Joan E. Strassmann, Washington University in St. Louis, St. Louis, MO, and approved October 16, 2017 (received for review June 29, 2017)

Some microbes possess the ability to adaptively manipulate host behavior. To better understand how such microbial parasites control animal behavior, we examine the cell-level interactions between the species-specific fungal parasite *Ophiocordyceps unilateralis sensu lato* and its carpenter ant host (*Camponotus castaneus*) at a crucial moment in the parasite's lifecycle: when the manipulated host fixes itself permanently to a substrate by its mandibles. The fungus is known to secrete tissue-specific metabolites and cause changes in host gene expression as well as atrophy in the mandible muscles of its ant host, but it is unknown how the fungus coordinates these effects to manipulate its host's behavior. In this study, we combine techniques in serial blockface scanning-electron microscopy and deep-learning–based image segmentation algorithms to visualize the distribution, abundance, and interactions of this fungus inside the body of its manipulated host. Fungal cells were found throughout the host body but not in the brain, implying that behavioral control of the animal body by this microbe occurs peripherally. Additionally, fungal cells invaded host muscle fibers and joined together to form networks that encircled the muscles. These networks may represent a collective foraging behavior of this parasite, which may in turn facilitate host manipulation.

deep learning | fungal networks | extended phenotype | behavioral manipulation | ants

Some parasitic microbes have evolved the ability to adaptively manipulate the behavior of the animals they infect (1). Examples include: unicellular Trypanosomes (class Kinetoplastida) that alter salivary composition and feeding behavior in tsetse flies, thereby increasing the parasite's transmission into mammalian hosts (2); fungi such as *Pandora* and *Ophiocordyceps* that induce ants to bite vegetation and die in an elevated location suitable for parasite dispersal (3–5); and the well-studied apicomplexan *Toxoplasma gondii*, which causes its rodent host to lose its innate fear of cats, enabling the parasite to transmit to the cat in which it reproduces (6). In each of these cases, the altered host behavior is an extended phenotype (7) of a microbial parasite's genes being expressed through the body of an animal. An important question to ask is how these microbes, which are much smaller than their hosts, can control animal behavior to produce such spectacular extended phenotypes. For example, an individual *T. gondii* parasite is less than 5 μm in diameter (8), whereas there are an estimated 4 million neurons in the mouse brain (9). However, because *T. gondii* can form "tissue cysts" containing the slowly multiplying stage, bradyzoite (8), successful host manipulation may rely on a collective behavior among the microbial parasites. One observation that supports this possibility is a correlation between the amount of dopamine released and the number of dopaminergic cells infected with *T. gondii*, which is known to produce tyrosine hydroxylase, the rate-limiting enzyme in dopamine synthesis (10).

Although correlated changes in chemical activity (or gene expression) between parasites and hosts are important, such evidence alone is likely insufficient to determine what role, if any, collective behavior among microbes plays during manipulation. Because of the size asymmetry between microbes and the hosts whose behavior they control, it is important to have a micrometer-level view of the interface between the microbe and the host tissue with which it interacts. Such an approach would complement studies on the chemical cross-talk between parasite and host, and it would allow us to better understand what role collective behavior among microbes may play during behavioral manipulation.

One promising model system for such detailed, micrometer-level studies is the entomopathogenic fungal parasite *Ophiocordyceps unilateralis sensu lato* (*s.l.*) and its ant host. The fungus *O. unilateralis s.l.* is a complex of species that are all obligate parasites of ants from the tribe Camponotini, notably *Camponotus* and *Polyrhachis* (5). A distinct advantage of this system is that the ants can be infected in the laboratory (11). As with other entomopathogenic fungi, species in the unilateralis complex enter their hosts by penetrating the cuticle to then proliferate and fill the ant's body (12). As such, the infection cycle begins when the parasite is a small free-floating cell in the open circulatory system of its insect host. After the required

Significance

Microbial parasites may behave collectively to manipulate their host's behavior. We examine adaptations of a microbial parasite in its natural environment: the body of its coevolved and manipulated host. Electron microscopy and 3D reconstructions of host and parasite tissues reveal that this fungus invades muscle fibers throughout the ant's body but leaves the brain intact, and that the fungal cells connect to form extensive networks. The connections are likened to structures that aid in transporting nutrients and organelles in several plant-associated fungi. These findings alter the current view of parasite-extended phenotypes by demonstrating that behavior control does not require the parasite to physically invade the host brain and that parasite cells may coordinate to change host behavior.

Author contributions: M.A.F. and D.P.H. designed research; M.A.F., Y.Z., R.G.L., C.A.M., D.Z.C., and D.P.H. performed research; Y.Z., M.L.H., and D.Z.C. contributed new reagents/analytic tools; M.A.F., Y.Z., and D.P.H. analyzed data; and M.A.F., Y.Z., C.A.M., D.Z.C., and D.P.H. wrote the paper.

The authors declare no conflict of interest.

This article is a PNAS Direct Submission.

Data deposition: Data generated in this study are available on Pennsylvania State University ScholarSphere, available at https://scholarsphere.psu.edu/concern/generic_works/6q524jn254.

[1]To whom correspondence should be addressed. Email: dhughes@psu.edu.

This article contains supporting information online at www.pnas.org/lookup/suppl/doi:10.1073/pnas.1711673114/-/DCSupplemental.

16–25 d of growth, the aggregation of microbial cells has reached the stage in which the fungus induces the ant to bite onto a plant in a location that is optimal for the fungus to grow and disperse (5, 13). This conspicuous biting behavior is an unambiguous signal of successful manipulation. Such modified behaviors that increase parasite transmission are not restricted to species in the *Ophiocordyceps* genus. The ability to manipulate ants to bite onto a plant in an elevated location has evolved in at least two other phylogenetically distant groups: the fungus *Pandora formicae* (phylum Entomophthoromycota) and the trematode *Dicrocoelium dendriticum*. Insights from the *O. unilateralis s.l.* system may therefore set the stage for future research on the convergent evolution of behavioral manipulation.

Previous work showed that *O. unilateralis s.l.* induces atrophy in mandible muscles of the worker ants manipulated to bite leaves (14), and this atrophy was suggested to play a role in the biting behavior. Both ex vivo metabolomic (11) and in vivo transcriptomic (13) studies suggested the fungus actively secretes small molecules that affect the muscles and nervous tissue. Although these approaches are informative, they provide only indirect observations of the parasite as it affects host muscles and ultimately host behavior, and they do not show how the individual cells of the parasite coordinate the manipulation. Additionally, at the same time when the muscles are atrophied, the brain seems to be preserved (13, 14), suggesting the parasite behaves differently toward distinct tissues. This is in line with the observation that entomopathogenic fungi secrete specific metabolites when cultured in the presence of muscle tissue or brain tissue (15). Such indirect approaches where gene activity or secreted chemicals are measured are useful, but direct observations of parasite and host cells would allow us to more precisely characterize how this fungus interacts with its ant host during manipulation.

In the present study, we directly observe fungal cells inside the manipulated host by integrating serial block-face scanning-electron microscopy (SEM) with automatic image segmentation and analyses that use deep-learning algorithms to distinguish host and parasite tissue in serial stacks of images. This approach allows us to examine the 3D structure and distribution of fungal cells in the muscle of manipulated ants. Because the atrophy reported in previous work (14) could be a general effect of fungal pathogenesis, we also infected ants with the generalist pathogen, *Beauveria bassiana*, which belongs to the same fungal order (Hypocreales) as *O. unilateralis s.l.* but does not manipulate its host as part of its lifecycle (16–18). This fungus thus serves as an important positive control, allowing us to begin to separate characteristics that are specific to the specialized insect/fungus interaction of *O. unilateralis s.l.* (typified by complex behavioral manipulation) from those effects on host tissue that result from general pathogenesis. We specifically aimed to describe the distribution, abundance, and interactions of *O. unilateralis s.l.* cells inside their host during manipulated biting behavior and to use these observations to hypothesize which fungal characteristics may play a role in producing this extended phenotype.

Results

The Fungus *O. unilateralis s.l.* Is Present Throughout the Body but Does Not Enter the Brain. Our first goal was to establish whether cells of the specialized fungus *O. unilateralis s.l.* were restricted to one location within the host ants. Previous work found a large aggregation of fungal cells in the head of manipulated ants, but other parts of the body were not examined (14). In the present study, we found *O. unilateralis s.l.* fungal cells in all three major body regions (head, thorax, and gaster; the latter is the ant-specific term for the terminal part of the abdomen) of the ant host ($n = 8$ *O. unilateralis s.l.*-infected ants) (Fig. S1). These fungal cells included two distinct forms: hyphal bodies, which are yeast-like cells that grow inside the insect body and multiply by budding (19), and hyphae, which are thin filamentous projections (collectively termed mycelia) that are specialized for foraging in new environments and invading host tissues (20, 21). In our study, hyphae grew exclusively from the ends of hyphal bodies (see, for example, Fig. 3*A*). We also found fungal cells in abundance inside the legs ($n = 12$ additional *O. unilateralis s.l.*-infected ants) (Fig. S2). Taken together, our data demonstrate that *O. unilateralis s.l.* is not restricted to the head of its host.

We also thoroughly examined the nervous tissue in the head for *O. unilateralis s.l.* cells to determine whether the fungus enters the brain of the ant it manipulates. Using fluorescence confocal microscopy, we tested for the presence of fungal cells within the host brain. In all samples [$n = 3$ per group (infected, uninfected)], fungal cells were concentrated directly outside the brain, but no fungal cells were observed inside the brain (Fig. 1).

Specialist and Generalist Fungal Pathogens Infiltrate Ant Muscle Tissue. We next wanted to determine the extent to which *O. unilateralis s.l.* invades the muscles of the ant it manipulates. Here we used the generalist pathogen, *B. bassiana*, as a positive control for host muscle responses during infection by a fungal pathogen. We used a Zeiss Sigma serial block-face SEM with Gatan 3View technology to examine 3D stacks of ant muscle. In these images, we observed muscular atrophy in ants infected by both species of fungi. This atrophy was characterized by large spaces between the muscle fibers (cells of muscle tissue) compared with uninfected samples.

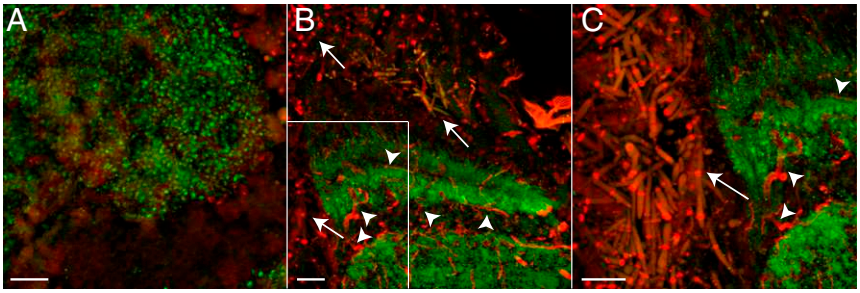

Fig. 1. Assessment of fungal invasion of the brain. Confocal images demonstrating the restriction of fungal invasion into the brain. Host brain is identified by immunofluorescence of neuronal synapses (green, anti-SYNORF1), while fungal cells and host tracheae are stained with calcofluor white (red, antichitin). All images are represented as maximum projections of *z*-stacks. (*A*) Portion of the mushroom body (green) in the brain of an uninfected (control) ant, 156× magnification. (Scale bar, 10 μm.) (*B*) Portion of the optic lobe (green) in the brain of an infected, behaviorally manipulated ant, 60× magnification. (Scale bar, 20 μm.) Arrows denote fungal hyphal bodies (red), identified by their short, rod-like structure and the presence of septa. Arrowheads denote tracheae (red), located within the brain (green), and identified by their long, filamentous structure and lack of septa. Note the restriction of fungal cell bodies to outside of the brain. (*C*) Zoom-in (96× magnification) of region of interest noted in *B*. (Scale bar, 20 μm.) While the presence of tracheae inside the brain is evident (arrowheads), there is no detection of fungal hyphal bodies (arrows) inside the brain.

Fungal cells of both species were present between the muscle fibers in both the head and leg regions (Fig. 2 *A*–*F*). We quantified the relative abundance of fungal tissue within the mandible muscle tissue using an image segmentation algorithm that we developed using deep learning (22) (*Materials and Methods*). We trained the algorithm to automatically distinguish between fungal and ant tissue from sequential 2D micrographs, which allowed us to quantify the volume of each tissue. We were then able to compare the difference in abundance between the two fungal species in the same ant species. Ants infected with *O. unilateralis s.l.* showed a median fungal abundance (volume of fungal tissue divided by combined volume of muscle and fungal tissue) of 10.06% (n = 8 ants, range = 4.09–38.19%) compared with a median of 2.09% (n = 8 ants, range = 0.30–52.28%) for ants infected with *B. bassiana* (Fig. 2 *G*–*I*). The distribution of abundances for these two fungal species was not significantly different (Wilcoxon rank-sum; $W = 16$, $n_1 = n_2 = 8$, $P = 0.1049$).

The Fungus *O. unilateralis s.l.* Forms Connections Between Hyphal Bodies and Invades Muscle Fibers. After demonstrating that fungal cells surround host muscle fibers (Fig. 2 *B*, *C*, *E*, *F*, *H*, and *I*), we investigated whether the fungal cells interact with each other and with the muscle fibers they surround. We discovered that many hyphal bodies of the specialist parasite *O. unilateralis s.l.* were connected to other hyphal bodies through short septated tubes ∼1-μm long (Fig. 3*B*, arrows, *Inset*). In fungi, such tubes are called conidial anastomosis tubes (CATs), which are specialized

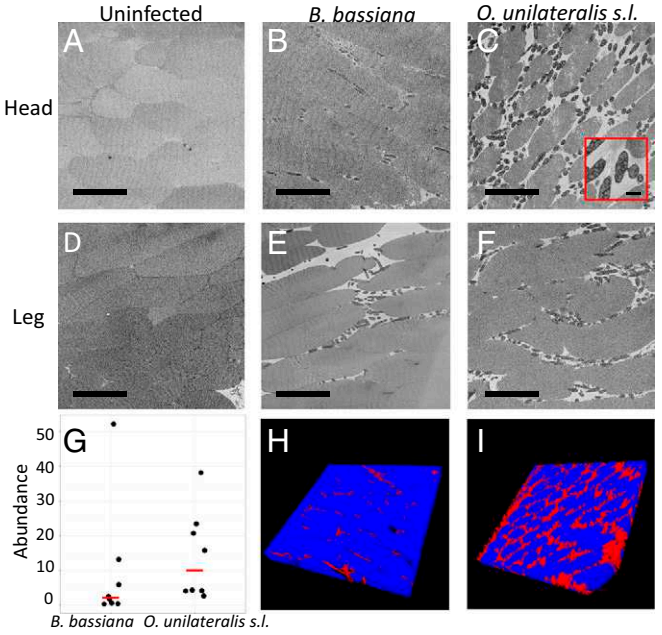

Fig. 2. Fungal abundance in muscle tissue. Serial block-face SEM images from three different ants representing the three treatment groups in this study. (*A*–*C*) Images from head samples (mandible adductor muscles); (*D*–*F*) images from leg samples (coxal levator or depressor muscles). *A* and *D* represent the control group (uninfected ants). Note that the muscle fibers are densely packed together. *B* and *E* represent ants infected with *B. bassiana*. Fungal cells (dark gray) are present between the muscle fibers. *C* and *F* represent ants infected with *O. unilateralis s.l*. Again, fungal cells are present between the muscle fibers, and some are connected via CATs (*Inset*). (Scale bars, 50 μm; *Inset*, 5 μm.) (*G*) The percent of fungal tissue (compared with total muscle and fungal tissue) over a volume of 100 serial block-face SEM slices. Each point represents one ant infected with either *B. bassiana* or *O. unilateralis s.l*. Red lines indicate medians. (*H* and *I*) Three-dimensional volume projections of two of the 100-image stacks used to obtain the abundance data in *G*. These projections were generated from the same samples as *B* and *C*, respectively.

hyphae that connect neighboring cells, allowing for transfer of cell contents between two conidia (23). Based on 3D SEM images (99 million μm^3 of ant tissue) and light micrographs (Fig. S2), we determined that the formation of CATs was commonly found in *O. unilateralis s.l.* in our study. However, we found no evidence of CATs between *B. bassiana* cells.

We also used the 3D SEM images to quantify the connections we observed in *O. unilateralis s.l.* When this specialist parasite first enters its host, it exists as free-floating cells in the open circulatory system. These cells then form connections via CATs, which implies communication between cells that leads to contact and cell wall fusion. We therefore wanted to determine how common CATs are for the specialist parasite. We examined 1,014 hyphal bodies of *O. unilateralis s.l.* and manually traced all connections between each focal cell and other cells to determine that 59% of hyphal bodies were connected to at least one other hyphal body (Fig. 3*D*). A single hyphal body could be attached to as many as six other hyphal bodies (mean connections per cell = 1.15, median = 1, n = 1,014, SD = 1.16). Qualitatively, connection rates were similar between the head and leg regions of the same ant (Fig. 3*D*).

Having established that hyphal bodies of *O. unilateralis s.l.* form extensive connections, we also quantified interactions of *O. unilateralis s.l.* fungal cells with the ant muscle fibers. Muscle fibers in all ants had *O. unilateralis s.l.* hyphal bodies directly touching their membrane, and in five of eight ants, hyphae had penetrated the membrane and entered the muscle cells (Fig. 3 *C* and *E*). The prevalence of this muscle fiber invasion varied widely between samples, with three of eight samples showing no invasion into any of the muscle cells examined (ants 6–8) (Fig. 2*E*). Muscle fiber invasion may have occurred in these ants, but we did not observe it in 99.9 million μm^3 of tissue.

Fungal Connections Create Extensive Networks. Because cellular interactions occur across space, and spatial relationships cannot be fully understood in two dimensions, we examined the 3D structure of the fungus in relation to the muscle fibers. We manually traced the edges of one muscle fiber and its neighboring hyphal bodies across 1,000 sequential micrographs that each measured 50 nm in depth. We discovered the cell–cell connections resulted in a 3D network of hyphal bodies that surrounded the muscle fiber (Fig. 4 and Movie S1). Both the 2D view (Fig. 3) and the 3D view (Fig. 4) show that some hyphal bodies do not touch host tissue, but they may still be connected to host cells via the fungal network to which they are attached. We quantified this and found 23% of the focal hyphal bodies we studied (234 of 1,014) did not touch any portion of the host muscle fiber directly. However, 75% of these cells (175 of 234) were connected to other hyphal bodies and may therefore have indirect contact to muscle fibers.

Discussion

This study reveals the distribution, abundance, and interactions of the specialized fungal parasite *O. unilateralis s.l.* within its natural habitat (the ant body) at a time in its lifecycle that is critical for its fitness: namely, when it induces its ant host to bite and die in a suitable microhabitat for the parasite's growth and dispersal (5, 24). By combining techniques in serial block-face SEM and deep-learning–based image segmentation and analysis, we directly observed and analyzed the 3D interactions between parasite and host cells at this crucial moment. In so doing, we revealed extensive connections among hyphal bodies as well as invasion of muscle fibers by hyphae. The connections between the hyphal bodies are called CATs, which are common among plant pathogenic fungi and are known to be involved in transfer of material between cells (23). By visualizing the fungal aggregation in 3D, we showed that hyphal bodies connected via CATs formed a network around muscle fibers of the host. The generalist fungal parasite *B. bassiana* did not form CATs and fungal networks inside the same ant species, which suggests such networks do not represent

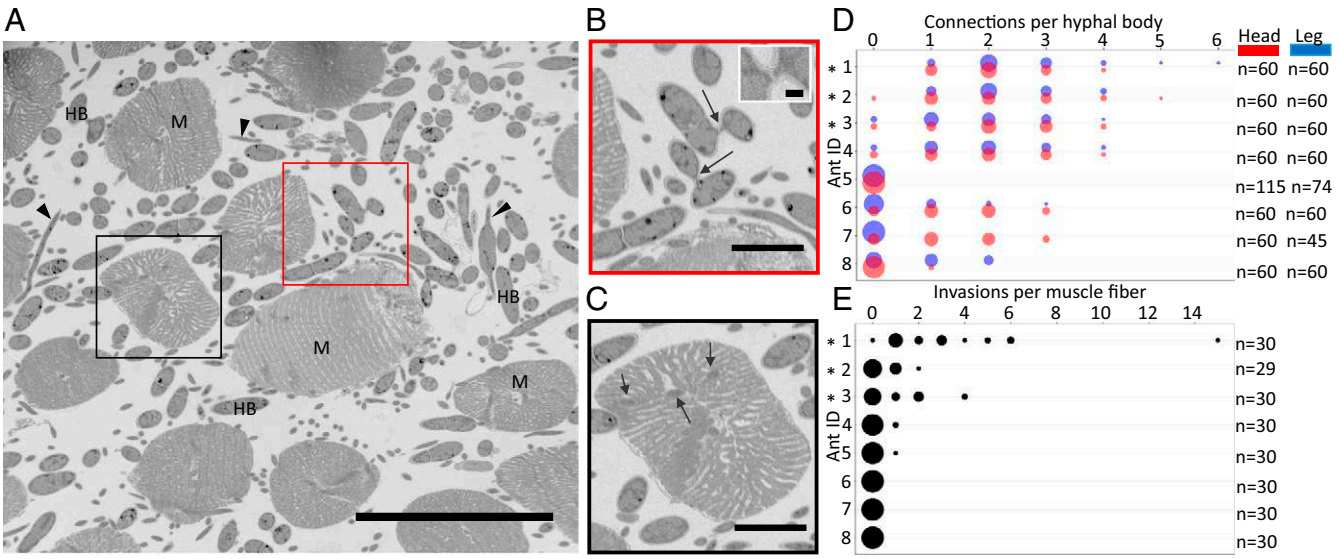

Fig. 3. Fungal interactions observed in *O. unilateralis s.l.*-infected ant muscles. (*A*) Serial block-face SEM image showing fungal hyphal bodies (HB) and hyphae (arrowheads) occupying the spaces between ant mandible muscle fibers (M). Outlined boxes are shown larger in *B* and *C*. (Scale bar, 50 μm.) (*B*) Connections between hyphal bodies (arrows). (Scale bar, 10 μm.) (*Inset*) Close-up of connected hyphal bodies. (Scale bar, 1 μm.) (*C*) Muscle fiber invasion: hyphae have penetrated the membrane of this muscle fiber and are embedded within the muscle cell (arrows). (Scale bar, 10 μm.) (*D*) Connections per hyphal body across leg and head regions for eight ants. Point sizes are proportional to number of occurrences. "*n*" refers to number of hyphal bodies sampled in each ant. (*E*) Invasions per muscle fiber (head only) across eight ants (same ants as in *D*). "*n*" refers to the number of muscle fibers examined in each ant. Asterisks (*) denote ants that were dead at the time of collection. Images from *A*–*C* were all taken from Ant #1.

a universal strategy of entomopathogenic fungi (though other entomopathogenic fungi must be examined with this technique). We suggest forming networks via CATs may be a specialized strategy that allows *O. unilateralis s.l.* to exploit its specific habitat (the body of its host) and continue its lifecycle.

Our first discovery was the apparent ubiquity of fungal cells throughout the host but a distinct absence in the brain. To manipulate its host, *O. unilateralis s.l.* requires precise control of mandible muscles, which are responsible for the final biting behavior (13, 14), so we expected fungal cells to be abundant in the head region (Fig. 2). However, we also expected to find fungal cells in the brain, which is presumably important for manipulation of host behavior. Instead, we found no evidence of *O. unilateralis s.l.* fungal cells in ant brains (Fig. 1), which supports suggestions from previous work (14). The manipulated biting behavior that typifies this system has convergently evolved in another fungus (4) and a trematode (1). The African liver fluke, *Dicrocoelium hospes* (class Trematoda), enters the ant's antennal lobes, and the congeneric species, *D. dendriticum*, enters the subesophageal ganglion, where it abuts mandibular nerves (25). In both cases, the ants ascend vegetation where they are eaten by ruminants, allowing the parasite to reproduce (1). But only with *D. dendriticum* are the ants induced to bite plant tissue (grasses), which is the suggested reason for the parasite to abut the mandibular nerves (25). The Entomophthoralean fungus *Pandora formicae* also induces infected ants to ascend and bite vegetation before death, but its position relative to the host's central nervous system during the biting behavior is unknown. In the *O. unilateralis s.l.* system, the absence of fungal cells in the brain implies the biting behavior does not require direct contact with the brain. The species of *O. unilateralis s.l.* studied here can dynamically alter the secondary metabolite profile it secretes in the presence of brain versus muscle tissue, and it also produces unique metabolites when it encounters a brain it normally manipulates compared with a brain from an ant species it does not control (11). Thus, the biting behavior may be driven by chemical means, and more work is needed to understand the effect of this specialist parasite given our observation that the brain is not invaded.

Although we found no evidence that *O. unilateralis s.l.* cells enter the host brain (Fig. 1), the cells were abundant in the rest of the head capsule and in other sections of the ant's body (Fig. S1), including the legs. This widespread distribution suggests that the fungus does not target a particular area that may be especially suitable for inducing the biting behavior. This finding contrasts with some other behavior-manipulating parasites, such as *Polypocephalus* sp., tapeworms, and *Dicrocoelium* sp., trematodes, which invade specific regions in the central nervous system of their hosts (shrimp and ants, respectively) (25, 26). The nonrandom localization of some parasites inside their hosts could be related to their ability to manipulate behavior (26).

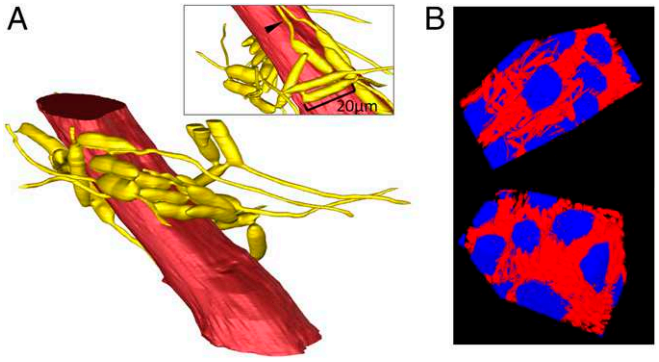

Fig. 4. Three-dimensional reconstructions of fungal networks surrounding muscle fibers. (*A*) A single fiber of an ant mandible adductor muscle (red) surrounded by 25 connected hyphal bodies (yellow). Connections between cells are visible as short tubes, and many cells have hyphae growing from their ends. Some of these hyphae have grown along and parallel to the muscle fiber (arrowhead in *Inset*). This reconstruction was created using Avizo software. See also Movie S1 and interactive 3D pdf (Fig. S3). (*B*) Two different projections of a 3D reconstruction showing several muscle fibers (blue) and fungal hyphal bodies (red) from the same area as seen in *A*. This reconstruction was created using a method (developed here) that uses a U-Net deep-learning model.

MICROBIOLOGY

However, it might also reflect an ability of some parasites, like tapeworms and trematodes, to actively move inside the animal, whereas others, like fungi, are moved around passively by the open circulatory system.

In addition to being distributed throughout the host body, fungal cells were present in the interstices between muscle fibers (Fig. 2). Healthy muscle is normally a tightly packed system of fibers with no spacing between the fibers (27). Previous work demonstrated that the mandibular muscles of ants infected with *O. unilateralis s.l.* exhibited a distinct atrophy that resulted in the formation of such spaces (14). However, it was not known whether this muscle atrophy and the high abundance of fungal cells between the muscle fibers were the results of specific adaptations of *O. unilateralis s.l.*, and thus related to a lifecycle that requires manipulation, or whether these changes were general effects of entomopathogens. In the present study, we therefore included the fungus *B. bassiana*, which does not manipulate behavior, as a positive control. This was a useful addition because it showed that cells of this generalist fungal pathogen also occupied the spaces between muscle cells. We expected that if fungal abundance and the related atrophy of host muscle were major factors in host manipulation, the specialist *O. unilateralis s.l.* might have had a higher abundance than *B. bassiana*. The finding that both fungal species were present and similarly abundant between the fibers implies the formation of the interstices is likely not a specific adaptation of the specialized behavior-manipulating fungus. It also suggests a shared mechanism of muscle degradation leading to separation of the fibers. Given the large energy reserves that muscles contain (in the form of mitochondria), both generalist and specialist entomopathogens may move into areas of high muscle density as part of their strategy to grow and eventually kill the host (both species can only reproduce from dead insects). Previous work showed a significant reduction in mitochondrial density in muscles of manipulated ants (14). Mitochondria are considered the power generators of the cells, so the myopathy we observed may be the result of fungal cells consuming the energy reserves of the muscle fibers. The genus *Ophiocordyceps* infects insects in 10 orders (including Hymenoptera, to which the ants belong) (18, 24), and it would be instructive to study other *Ophiocordyceps* species as well as generalist fungal parasites to determine their effect on muscles of different insect hosts.

Not only did fungal cells enter muscle bundles, they also penetrated the muscle fibers themselves. Since the first step in colonizing the host body is the hyphal body stage, the appearance of the cell-invading mycelial phenotype implies a transition during which hyphae grow from one or both poles of the hyphal body (Fig. 2*A*, arrowheads). In fungi, the mycelium is the vegetative growth stage involved in foraging, resource acquisition, and accessing new environments. Typified by the secretion of enzymes at the polar region and subsequent cell wall synthesis localized to a surface of just a few micrometers, growing hyphae can penetrate substances that hyphal bodies cannot (28). An extreme example of such activity occurs in rock-eating fungi (29), but fungi routinely degrade cellulose and other recalcitrant biological material (30). We suggest the transition to apical growth from hyphal bodies allows the fungal community to access resources inside muscle cells, but other functions are also possible. The penetration of muscle cells by hyphae also occurred, albeit rarely, in ants infected by the generalist parasite, *B. bassiana*, so muscle cell invasion may represent a general strategy that future work should explore.

A fungal characteristic that we only observed in the specialist pathogen *O. unilateralis s.l.* was the formation of complex 3D networks surrounding the muscle fibers (Fig. 4, Fig. S3, and Movie S1). The networks consisted of many hyphal bodies joined by connections between the cell walls. The connections are known as CATs, which have been observed in 73 species (21 genera) of fungi (23). These fungal species in which CATs have been described are pathogens of plants, and here we show similar connections in a fungus infecting an animal. One possible function of the connections and network formation is suggested by our 3D reconstruction of 25 connected hyphal bodies surrounding a single muscle fiber (Fig. 4, Fig. S3, and Movie S1). Visualizing the network in this way allowed us to observe its size and shape. We determined that many hyphal bodies (23%, 234 of 1,014) did not directly touch the muscle fiber, but through their connections in the network they could still interact indirectly with the muscle fiber. One suggestion from these observations is that hyphae sequester resources from the muscles, and the connections between hyphal bodies allow nutrients to be transported to cells not directly touching the host. Studies on ectomycorrhizal fungal networks show that carbon can be transferred from one tree to another along extensive underground networks (31). Therefore, hyphal body networks could allow the fungus to acquire resources from muscles and distribute these resources to other fungal cells that are in the network but distant from the muscles.

In summary, we have shown, through the use of serial block-face SEM and automated image segmentation and analysis based on a deep-learning model, the 3D structure of a microbial parasite at the cellular level inside the body of its host. We demonstrated that during the critical biting behavior of manipulated ants, the specialist fungus *O. unilateralis s.l.* is present throughout the ant's body but not in the brain. The fungus takes the form of hyphal bodies that connect to form fungal networks, and it is also present as filamentous mycelia that invade ant muscle fibers. The connections between hyphal bodies indicate that individual fungal cells communicate with each other and suggest that collective behavior may be an important strategy for this fungal parasite. We speculate that the resulting networks may aid in nutrient transport and formation of the structures that will later emerge from the host's body to continue the parasite's lifecycle. Future work should continue to examine fungal behavior at the cellular level over the period of infection and across multiple areas within the ant's body.

Materials and Methods

Infection and Sample Collection. Ant and fungal colonies were maintained in the laboratory following procedures detailed in *SI Materials and Methods*. Colonies of the ant *Camponotus castaneus* were collected in Abbeville County, South Carolina (georeference: 34.375215, −82.346937) in July 2014. Cultures of *O. unilateralis s.l.* (Strain SC09B, also collected in Abbeville County) were grown from ascospores (sexually produced spores of Ascomycete fungi) since July 2014. Manipulated ants were collected following artificial infection with fungal material as described previously (11). Briefly, ants were injected under one foreleg with 1 μL of a fungal suspension (either fresh ascospores at 1×10^5 spores per milliliter or 1 cm^2 of cultured fungal material suspended in 500 μL of Grace's medium) and kept at high humidity with access to 10% sugar water ad libitum until collection (15–39 d after infection). It is unknown how many spores enter the ant during a natural infection and whether those spores are clonal or not. While our injection method may result in a different disease progression than what occurs in nature, the relevant outcome for our study is the induced biting behavior in the host, and this occurs both in the field and in the laboratory. In total, 23 manipulated ants (8 for histology and SEM, 3 for immunofluorescence, 12 for leg dissections) were collected from three rounds of infection. Collected ants displayed a characteristic biting behavior: they had been biting onto one of several available substrates in the cage for at least 10 min (no more than 12 h) at the time of collection. Control ants were not injected with fungus but were housed with infected ants and exposed to the same laboratory conditions. Ants infected with *B. bassiana* were surface-infected with 2 μL or 3 μL of spore suspension (10^8 or 10^9 spores per milliliter). Eight infected ants from two colonies were collected between 3 and 5 d after infection when ants were moribund (32) or within 1 h after death. Collected ants were either dissected immediately and fixed (for EM: 2.5% glutaraldehyde, 2% formaldehyde, 2 mM calcium chloride in 0.15 M cacodylate buffer, pH 7.4; for immunohistochemistry: 4% paraformaldehyde in PBS) or flash-frozen in liquid nitrogen and stored at −80 °C to be thawed, dissected, and fixed at a later date.

Immunofluorescence of Neural Tissue. Immunofluorescence assays were performed similar to previously described work (33, 34). Briefly, fixed ant heads were washed in PBS, cryoprotected (10/15/20% sucrose in PBS for 2 h each), and embedded in O.C.T. Heads were cut into 50-μM sections along the

transverse plane using a cryostat (Leica Biosystems), and mounted slides were postfixed briefly in 2% paraformaldehyde. Sections were rinsed with PBS, blocked and permeabilized in 10% donkey serum (Jackson ImmunoResearch) diluted in 0.1% Triton X-100/PBS. Slides were then incubated with primary antibody (3C11 anti-SYNORF1, 1:50, DSHB) overnight at 4 °C, washed, and then incubated in secondary antibody [Alexa Fluor 488 AffiniPure F(ab′)$_2$ fragment donkey anti-mouse IgG (H+L), 1:200; Jackson ImmunoResearch] and calcofluor white antichitin stain (1:100; Sigma-Aldrich). Sections were then washed and mounted in ProLong Gold (ThermoFisher Scientific) and imaged using a confocal laser scanning microscope (Olympus FluoView FV10i) and a 60× water immersion objective. All images are presented as maximum projections of *z*-stacks. Background subtraction was performed using the rolling ball method (radius = 50) in ImageJ. Brightness and contrast were adjusted equally for all images using PhotoShop (Adobe).

Serial Block-Face SEM. The right half of the head and one forecoxa from each ant were prepared for serial block-face SEM according to the protocol of the National Center for Microscopy and Imaging Research, University of California, San Diego (35). Pin-mounted samples were sectioned using a serial block-face SEM (Gatan 3View on Zeiss SIGMA VP-FESEM) at 50- or 100-nm thickness. Approximately 120 μm of tissue was sliced (1,200 or 2,400 slices) from each *O. unilateralis s.l.* sample and 10 μm (100 slices) from *B. bassiana* and control samples. Digital Micrograph (Gatan) software was used to align image stacks and quantify interactions between cells (for details of quantification, see *SI Materials and Methods*). Image segmentation and 3D reconstruction were performed using a deep-learning model (see below) as well as the programs Avizo and Amira (FEI). Model smoothing and 3D pdf generation were performed with help from Thomas van de Kamp, Karlsruhe Institute of Technology, Karlsruhe, Germany, as described previously (36).

Deep-Learning Model for Image Segmentation. The automated image segmentation used to compute the relative abundance of fungus and muscle tissue in each sample was performed using a model developed by Zhang et al. (22). To perform quantitative analysis, our first step was to segment the image data. In recent years, fully convolutional networks have shown highly promising results in semantic segmentation (37). Our segmentation problem can be viewed as a special case of general semantic segmentation. Compared with natural scene images, the number of classes in our images is much smaller, but the size of our training data is quite limited. Thus, our approach must be different from the original fully convolutional networks, which were designed for general computer vision tasks. U-Net (38) is a specially designed fully convolutional network for segmenting biomedical image data, and we applied this model for automatic fungus and muscle segmentation. For each stack, we manually labeled two sections to train the model and then applied the trained model to the remaining sections. We stacked the segmentation results for all sections to form the 3D segmentation. To calculate the segmentation accuracy, we compared the model results with ground truth data (one section from each stack marked by a human expert). For simpler stacks, the F1 score is over 96%, and for harder stacks, the F1 score is over 93% (voxel level). Based on the segmentation, we used a computer program to count voxels of fungi, muscles, and other areas, and we calculated the volume ratios for each pair accordingly.

Data generated in this study are available on Pennsylvania State University ScholarSphere (https://scholarsphere.psu.edu/concern/generic_works/6q524jn254).

ACKNOWLEDGMENTS. We thank Kim Fleming for inviting us to collect ants and fungus on her land; Nina Jenkins (Pennsylvania State University) for providing spores of *Beauveria Bassiana*; Greg Ning and John Cantolina (Pennsylvania State University Microscopy and Cytometry Facility) for assistance with microscopy and sample preparation; undergraduate assistant Saad Ahmad (Pennsylvania State University) for digitizing histology slides; and the Huck Institutes of the Life Sciences for microscopy facilities and logistical support. The SYNORF1 antibody, developed by Erich Buchner, was obtained from the Developmental Studies Hybridoma Bank, created by the National Institute of Child Health and Human Development of the NIH and maintained at the University of Iowa, Department of Biology. This work was supported in part by National Science Foundation Grants IOS-1558062 (to D.P.H.), CCF-1217906 (to D.Z.C.), CNS-1629914 (to D.Z.C.), and CCF-1617735 (to D.Z.C.); and NIH Grant R01 GM116927-02 (to D.P.H., D.C.Z., M.A.F., and Y.Z.). R.G.L. was funded by Comissao de Aperfeiçoamento de Pessoal de Nival Superior-Brazil (Project 6203-10-8). C.A.M. was funded by the American Heart Association (16POST29920001).

1. Moore J (2002) *Parasites and the Behavior of Animals* (Oxford Univ Press, Oxford, UK).
2. Van Den Abbeele J, Caljon G, De Ridder K, De Baetselier P, Coosemans M (2010) *Trypanosoma brucei* modifies the tsetse salivary composition, altering the fly feeding behavior that favors parasite transmission. *PLoS Pathog* 6:e1000926.
3. Marikovsky PI (1962) On some features of behavior of the ants *Formica rufa* L. infected with fungus disease. *Insectes Soc* 9:173–179.
4. Małagocka J, Grell MN, Lange L, Eilenberg J, Jensen AB (2015) Transcriptome of an entomophthoralean fungus (*Pandora formicae*) shows molecular machinery adjusted for successful host exploitation and transmission. *J Invertebr Pathol* 128:47–56.
5. Andersen SB, et al. (2009) The life of a dead ant: The expression of an adaptive extended phenotype. *Am Nat* 174:424–433.
6. Berdoy M, Webster JP, Macdonald DW (2000) Fatal attraction in rats infected with *Toxoplasma gondii*. *Proc Biol Sci* 267:1591–1594.
7. Dawkins R (1982) *The Extended Phenotype* (Oxford Univ Press, Oxford, UK).
8. Dubey JP, Lindsay DS, Speer CA (1998) Structures of *Toxoplasma gondii* tachyzoites, bradyzoites, and sporozoites and biology and development of tissue cysts. *Clin Microbiol Rev* 11:267–299.
9. Roth G, Dicke U (2005) Evolution of the brain and intelligence. *Trends Cogn Sci* 9: 250–257.
10. Prandovszky E, et al. (2011) The neurotropic parasite *Toxoplasma gondii* increases dopamine metabolism. *PLoS One* 6:e23866.
11. de Bekker C, et al. (2014) Species-specific ant brain manipulation by a specialized fungal parasite. *BMC Evol Biol* 14:166.
12. Charnley AK (1989) Mechanisms of fungal pathogenesis in insects. *Biotechnology of Fungi for Improving Plant Growth*, eds Whipps JM, Lumsen RD (Cambridge Univ Press, Cambridge, UK), pp 85–125.
13. de Bekker C, et al. (2015) Gene expression during zombie ant biting behavior reflects the complexity underlying fungal parasitic behavioral manipulation. *BMC Genomics* 16:620.
14. Hughes DP, et al. (2011) Behavioral mechanisms and morphological symptoms of zombie ants dying from fungal infection. *BMC Ecol* 11:13.
15. de Bekker C, Smith PB, Patterson AD, Hughes DP (2013) Metabolomics reveals the heterogeneous secretome of two entomopathogenic fungi to ex vivo cultured insect tissues. *PLoS One* 8:e70609.
16. Roy HE, Steinkraus DC, Eilenberg J, Hajek AE, Pell JK (2006) Bizarre interactions and endgames: Entomopathogenic fungi and their arthropod hosts. *Annu Rev Entomol* 51:331–357.
17. Humber RA (2008) Evolution of entomopathogenicity in fungi. *J Invertebr Pathol* 98: 262–266.
18. Araújo JPM, Hughes DP (2016) Diversity of entomopathogenic fungi: Which groups conquered the insect body? *Adv Genet* 94:1–39.
19. Prasertphon S, Tanada Y (1968) Formation and circulation, in Galleria, of hyphal bodies of entomophthoraceous fungi. *J Invertebr Pathol* 11:260–280.
20. Kirk P, Cannon P, Minter D, Stalpers J (2008) *Ainsworth & Bisby's Dictionary of the Fungi* (CAB International, Wallingford, UK), 10th Ed.
21. Boucias DG, Pendland JC (1998) General Properties of fungal pathogens. *Principles of Insect Pathology* (Springer, New York), pp 259–286.
22. Zhang Y, et al. (2017) Deep adversarial networks for biomedical image segmentation utilizing unannotated images. *Medical Image Computing and Computer Assisted Intervention* (Springer, Cham, Switzerland), pp 408–416.
23. Gabriela Roca M, Read ND, Wheals AE (2005) Conidial anastomosis tubes in filamentous fungi. *FEMS Microbiol Lett* 249:191–198.
24. Hughes DP, et al. (2016) From so simple a beginning: The evolution of behavioral manipulation by fungi. *Adv Genet* 94:437–469.
25. Romig T, Lucius R, Frank W (1980) Cerebral larvae in the second intermediate host of *Dicrocoelium dendriticum* (Rudolphi, 1819) and *Dicrocoelium hospes* Looss, 1907 (Trematodes, Dicrocoeliidae). *Z Parasitenkd* 63:277–286.
26. Carreon N, Faulkes Z (2014) Position of larval tapeworms, *Polypocephalus* sp., in the ganglia of shrimp, *Litopenaeus setiferus*. *Integr Comp Biol* 54:143–148.
27. Paul J (2001) Mandible movements in ants. *Comp Biochem Physiol A Mol Integr Physiol* 131:7–20.
28. Read ND (2011) Exocytosis and growth do not occur only at hyphal tips. *Mol Microbiol* 81:4–7.
29. Jongmans AG, et al. (1997) Rock-eating fungi. *Nature* 389:682–683.
30. Cragg SM, et al. (2015) Lignocellulose degradation mechanisms across the Tree of Life. *Curr Opin Chem Biol* 29:108–119.
31. Klein T, Siegwolf RTW, Körner C (2016) Belowground carbon trade among tall trees in a temperate forest. *Science* 352:342–344.
32. Heinze J, Walter B (2010) Moribund ants leave their nests to die in social isolation. *Curr Biol* 20:249–252.
33. Gao Q, Yuan B, Chess A (2000) Convergent projections of *Drosophila* olfactory neurons to specific glomeruli in the antennal lobe. *Nat Neurosci* 3:780–785.
34. Vanguilder HD, Bixler GV, Sonntag WE, Freeman WM (2012) Hippocampal expression of myelin-associated inhibitors is induced with age-related cognitive decline and correlates with deficits of spatial learning and memory. *J Neurochem* 121:77–98.
35. Deerinck T, Bushong E, Thor A, Ellisman M (2010) NCMIR Methods for 3D EM: A New Protocol for Preparation of Biological Specimens for Serial Block Face Scanning Electron Microscopy (National Center for Microscopy and Imaging Research, La Jolla), Version 7_01_10.
36. van de Kamp T, dos Santos Rolo T, Vagovič P, Baumbach T, Riedel A (2014) Three-dimensional reconstructions come to life—Interactive 3D PDF animations in functional morphology. *PLoS One* 9:e102355.
37. Shelhamer E, Long J, Darrell T (2017) Fully convolutional networks for semantic segmentation. *IEEE Trans Pattern Anal Mach Intell* 39:640–651.
38. Ronneberger O, Fischer P, Brox T (2015) U-Net: Convolutional networks for biomedical image segmentation. *MICCAI* (Springer, Cham, Switzerland), pp 234–241.